

Unfolding Projection-free SDP Relaxation of Binary Graph Classifier via GDPA Linearization

Cheng Yang[†], Gene Cheung[‡], Wai-tian Tan[§], Guangtao Zhai[†]

[†] Shanghai Jiaotong University, Shanghai, China [‡] York University, Toronto, Canada [§] Cisco Systems, San José, CA

Abstract

Algorithm unfolding creates an interpretable and parsimonious neural network architecture by implementing each iteration of a model-based algorithm as a neural layer. However, unfolding a proximal splitting algorithm with a positive semi-definite (PSD) cone projection operator per iteration is expensive, due to the required full matrix eigen-decomposition. In this paper, leveraging a recent linear algebraic theorem called Gershgorin disc perfect alignment (GDPA), we unroll a projection-free algorithm for semi-definite programming relaxation (SDR) of a binary graph classifier, where the PSD cone constraint is replaced by a set of “tightest possible” linear constraints per iteration. As a result, each iteration only requires computing a linear program (LP) and one extreme eigenvector. Inside the unrolled network, we optimize parameters via stochastic gradient descent (SGD) that determine graph edge weights in two ways: i) a metric matrix that computes feature distances, and ii) a sparse weight matrix computed via local linear embedding (LLE). Experimental results show that our unrolled network outperformed pure model-based graph classifiers, and achieved comparable performance to pure data-driven networks but using far fewer parameters.

INTRODUCTION

While generic and powerful *deep neural networks* (DNN) (LeCun, Bengio, and Hinton 2015) can achieve state-of-the-art performance using large labelled datasets for many data-fitting problems such as image restoration and classification (Zhang et al. 2017; Krizhevsky, Sutskever, and Hinton 2012), they operate as “black boxes” that are difficult to explain. To build an interpretable system targeting a specific problem instead, *algorithm unfolding* (Monga, Li, and Eldar 2021) takes a model-based iterative algorithm, implements (unrolls) each iteration as a neural layer, and stacks them in sequence to compose a network architecture. As a pioneering example, LISTA (Gregor and LeCun 2010) implemented each iteration of a sparse coding algorithm called ISTA (Beck and Teboulle 2009)—composed of a gradient descent step and a soft thresholding step—as linear and ReLU operators in a neural layer. By optimizing two matrix parameters in the linear operator per layer end-to-end via *stochastic gradient descent* (SGD)

Preprint. Under review.

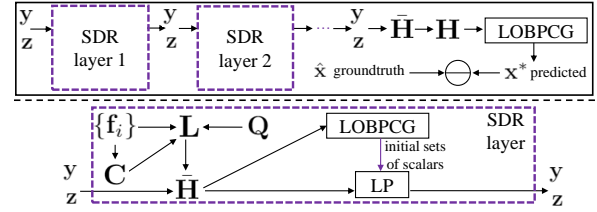


Figure 1: Overview of our SDP relaxation (SDR) network. Upper: SDR network composed of stacked SDR layers. Lower: The architecture of a single SDR layer. The lower triangular matrix \mathbf{Q} and local linear embedding (LLE) weight matrix \mathbf{C} are used to define the conically combined Laplacian matrix \mathbf{L} , which is then used together with the SDP dual variables \mathbf{y} and \mathbf{z} to define the matrix $\bar{\mathbf{H}}$. Next, $\bar{\mathbf{H}}$ is passed to differentiable LOBPCG solver and LP solver to update \mathbf{y} and \mathbf{z} . The network is end-to-end trained with an MSE loss of the predicted labels.

(Bottou 1998), LISTA converged faster and had better performance. This means that the required iteration / neural layer count was comparatively small, resulting in a parsimonious architecture with few learned network parameters.

However, algorithm unfolding is difficult if the iterative algorithm performs *proximal splitting* (Boyd et al. 2011) with a *positive semi-definite* (PSD) cone projection operator per iteration; PSD cone projection is common in algorithms solving a *semi-definite programming* (SDP) problem with a PSD cone constraint (Gartner and Matousek 2012). A PSD cone projection for a matrix variable \mathbf{H} requires full matrix eigen-decomposition on \mathbf{H} with complexity $\mathcal{O}(N^3)$. Not only is the computation cost of the projection in a neural layer expensive, optimizing network parameters through the projection operator via SGD is difficult.

In this paper, using binary graph classifier (Zhou et al. 2003; Belkin, Matveeva, and Niyogi 2004; Guillory and Bilmes 2009; Luo et al. 2010) as an illustrative application, we demonstrate how PSD cone projection can be entirely circumvented for an SDP problem, facilitating algorithm unfolding and end-to-end optimization of network parameters without sacrificing performance. Specifically, we first replace the PSD cone constraint in the original *semi-definite programming relaxation* (SDR) (Li, Liu, and Tang 2008) of

the NP-hard graph classifier problem with “tightest possible” linear constraints per iteration, thanks to a recent linear algebraic theorem called *Gershgorin disc perfect alignment* (GDPA) (Yang, Cheung, and Hu 2021). Together with the linear objective, each iteration computes only a *linear program* (LP) (Vanderbei 2021) and one extreme eigenvector (computable in $\mathcal{O}(N)$ using LOBPCG (Knyazev 2001)).

We next unroll the now projection-free iterative algorithm into an interpretable network, and optimize parameters that determine graph edge weights per neural layer via SGD in two ways. First, assuming edge weight $w_{i,j}$ is inversely proportional to *feature distance* $d_{i,j}$ between nodes i and j endowed with feature vectors \mathbf{f}_i and \mathbf{f}_j respectively, we optimize a PSD metric matrix \mathbf{M} via Cholesky factorization (Golub and Van Loan 1996) $\mathbf{M} = \mathbf{Q}\mathbf{Q}^\top$ that computes *Mahalanobis distance* (Mahalanobis 1936) as $d_{i,j} = (\mathbf{f}_i - \mathbf{f}_j)^\top \mathbf{M}(\mathbf{f}_i - \mathbf{f}_j)$. Second, we initialize a non-negative symmetric weight matrix via *local linear embedding* (LLE) (Roweis and Saul 2000; Ghogogh et al. 2020) given feature vectors \mathbf{f}_i ’s, which we subsequently fine-tune per layer in a semi-supervised manner. We employ a conic combination of the two resulting graph Laplacian matrices for classification in each layer. An illustration of the unrolled network is shown in Fig. 1.

We believe this methodology of replacing the PSD cone constraint by linear constraints per iteration—leading to an iterative algorithm amenable to algorithm unfolding—can be more generally applied to a broad class of SDP problems with PSD cone constraints (Gartner and Matousek 2012). For binary graph classifiers, experimental results show that our interpretable unrolled network substantially outperformed pure model-based classifiers (Yang et al. 2021), and achieved comparable performance as pure data-driven networks (Le-Cun, Bengio, and Hinton 2015) but using noticeably fewer parameters.

RELATED WORK

Algorithm unfolding is one of many classes of approaches in *model-based deep learning* (Shlezinger et al. 2021), and has been shown effective in creating interpretable network architectures for a range of data-fitting problems (Monga, Li, and Eldar 2021). We focus on unfolding of iterative algorithms involving PSD cone projection (O’Donoghue et al. 2016) that are common when addressing SDR of NP-hard *quadratically constrained quadratic programming* (QCQP) problems (Luo et al. 2010), of which binary graph classifier is a special case.

Graph-based classification was first studied two decades ago (Zhou et al. 2003; Belkin, Matveeva, and Niyogi 2004; Guillory and Bilmes 2009). An interior point method tailored for the slightly more general *binary quadratic problem*¹ (BQP) has complexity $\mathcal{O}(N^{3.5} \log(1/\epsilon))$, where ϵ is the tolerable error (Helmsberg et al. 1996). Replacing PSD cone constraint $\mathbf{M} \succeq 0$ with a factorization $\mathbf{M} = \mathbf{X}\mathbf{X}^\top$ was proposed (Shah et al. 2016), but it resulted in a non-convex optimization for \mathbf{X} that was solved locally via alternating minimization, where in each iteration a matrix inverse of worst-case complexity $\mathcal{O}(N^3)$ was required. More recent

¹BQP objective takes a quadratic form $\mathbf{x}^\top \mathbf{Q}\mathbf{x}$, but \mathbf{Q} is not required to be a Laplacian matrix to a similarity graph.

first-order methods such as (O’Donoghue et al. 2016) used ADMM (Boyd et al. 2011), but still requires expensive PSD cone projection per iteration. In contrast, leveraging GDPA theory (Yang, Cheung, and Hu 2021), our algorithm is entirely projection-free.

GDPA theory was developed for *metric learning* (Moutafis, Leng, and Kakadiaris 2017) to optimize a PD *metric matrix* \mathbf{M} , given a convex and differentiable objective $Q(\mathbf{M})$, in a Frank-Wolfe optimization framework (Jaggi 2013). This paper leverages GDPA (Yang, Cheung, and Hu 2021) in an entirely different direction for unfolding of a projection-free graph classifier learning algorithm.

PRELIMINARIES

Graph Definitions

A graph is defined as $\mathcal{G}(\mathcal{V}, \mathcal{E}, \mathbf{W})$, with node set $\mathcal{V} = \{1 \dots, N\}$, and edge set $\mathcal{E} = \{(i, j)\}$, where (i, j) means nodes i and j are connected with weight $w_{i,j} \in \mathbb{R}$. A node i may have a self-loop of weights $u_i \in \mathbb{R}$. Denote by \mathbf{W} the *adjacency matrix*, where $W_{i,j} = w_{i,j}$ and $W_{i,i} = u_i$. We assume that edges are undirected, and \mathbf{W} is symmetric. Define next the diagonal *degree matrix* \mathbf{D} , where $D_{i,i} = \sum_j W_{i,j}$. The *combinatorial graph Laplacian matrix* (Ortega et al. 2018) is then defined as $\mathbf{L} \triangleq \mathbf{D} - \mathbf{W}$. To account for self-loops, the *generalized graph Laplacian matrix* is defined as $\mathcal{L} \triangleq \mathbf{D} - \mathbf{W} + \text{diag}(\mathbf{W})$. Note that any real symmetric matrix can be interpreted as a generalized graph Laplacian matrix.

The *graph Laplacian regularizer* (GLR) (Pang and Cheung 2017) that quantifies smoothness of signal $\mathbf{x} \in \mathbb{R}^N$ w.r.t. graph specified by \mathcal{L} is

$$\mathbf{x}^\top \mathcal{L}\mathbf{x} = \sum_{(i,j) \in \mathcal{E}} w_{i,j} (x_i - x_j)^2 + \sum_{i \in \mathcal{V}} u_i x_i^2. \quad (1)$$

GLR is also the objective of our graph-based classification problem.

GDPA Linearization

To ensure matrix variable \mathbf{M} is PSD without eigen-decomposition, we leverage GDPA (Yang, Cheung, and Hu 2021). Given a real symmetric matrix, we define a *Gershgorin disc* Ψ_i corresponding to row i of \mathbf{M} with center $c_i(\mathbf{M}) \triangleq M_{i,i}$ and radius $r_i(\mathbf{M}) \triangleq \sum_{j \neq i} |M_{i,j}|$. By *Gershgorin Circle Theorem* (GCT) (Varga 2004), the smallest real eigenvalue $\lambda_{\min}(\mathbf{M})$ of \mathbf{M} is lower-bounded by the smallest disc left-end $\lambda_{\min}^-(\mathbf{M})$, i.e.,

$$\lambda_{\min}^-(\mathbf{M}) \triangleq \min_i c_i(\mathbf{M}) - r_i(\mathbf{M}) \leq \lambda_{\min}(\mathbf{M}). \quad (2)$$

Thus, to ensure $\mathbf{M} \succeq 0$, one can impose the sufficient condition $\lambda_{\min}^-(\mathbf{M}) \geq 0$, or equivalently

$$c_i(\mathbf{M}) - r_i(\mathbf{M}) \geq 0, \quad \forall i. \quad (3)$$

However, GCT lower bound $\lambda_{\min}^-(\mathbf{M})$ tends to be loose. As an example, consider the *positive definite* (PD) matrix \mathbf{M} in Fig. 2 with $\lambda_{\min}(\mathbf{M}) = 0.1078$. The first disc left-end is $c_1(\mathbf{M}) - r_1(\mathbf{M}) = 2 - 3 = -1$, and $\lambda_{\min}^-(\mathbf{M}) < 0$.

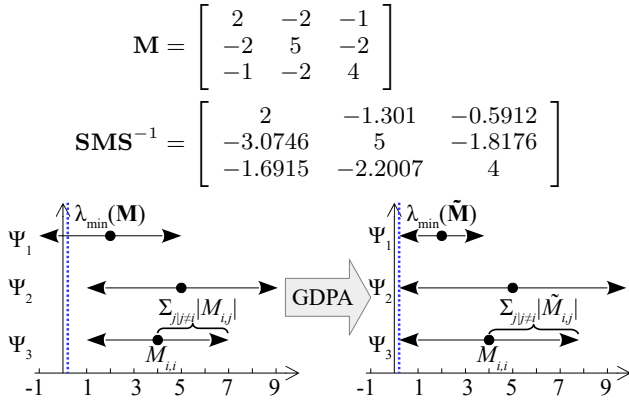


Figure 2: Example of a PD matrix \mathbf{M} and its similarity transform $\tilde{\mathbf{M}} = \mathbf{SMS}^{-1}$, and their respective Gershgorin discs Ψ_i . Gershgorin disc left-ends of $\tilde{\mathbf{M}}$ are aligned at $\lambda_{\min}(\mathbf{M}) = 0.1078$.

GDPA provides a theoretical foundation to tighten the GCT lower bound. Specifically, GDPA states that given a generalized graph Laplacian matrix \mathbf{M} corresponding to a “balanced” signed graph² \mathcal{G} (Cartwright and Harary 1956), one can perform a *similarity transform*³, $\tilde{\mathbf{M}} = \mathbf{SMS}^{-1}$, where $\mathbf{S} = \text{diag}(v_1^{-1}, \dots, v_N^{-1})$ and \mathbf{v} is the first eigenvector of \mathbf{M} , such that all the disc left-ends of $\tilde{\mathbf{M}}$ are exactly aligned at $\lambda_{\min}(\mathbf{M}) = \lambda_{\min}(\tilde{\mathbf{M}})$. This means that transformed $\tilde{\mathbf{M}}$ satisfies $\lambda_{\min}^-(\tilde{\mathbf{M}}) = \lambda_{\min}(\tilde{\mathbf{M}})$; *i.e., the GCT lower bound is the tightest possible after an appropriate similarity transform*. Continuing our example, similarity transform $\tilde{\mathbf{M}} = \mathbf{SMS}^{-1}$ of \mathbf{M} has all its disc left-ends exactly aligned at $\lambda_{\min}(\mathbf{M}) = \lambda_{\min}(\tilde{\mathbf{M}}) = 0.1078$.

Leveraging GDPA, (Yang, Cheung, and Hu 2021) developed a fast metric learning algorithm, in which the PSD cone constraint $\mathbf{M} \succeq 0$ is replaced by linear constraints $\lambda_{\min}^-(\mathbf{S}_t \mathbf{M} \mathbf{S}_t^{-1}) \geq 0$ per iteration, where $\mathbf{S}_t = \text{diag}(v_1^{-1}, \dots, v_N^{-1})$ and \mathbf{v} is the first eigenvector of previous solution \mathbf{M}_{t-1} . Assuming that the algorithm always seeks solutions \mathbf{M} in the space of graph Laplacian matrices of balanced graphs, this means previous PSD solution \mathbf{M}_{t-1} remains feasible at iteration t , since by GDPA $\lambda_{\min}^-(\mathbf{S}_t \mathbf{M}_{t-1} \mathbf{S}_t^{-1}) = \lambda_{\min}(\mathbf{M}_{t-1}) \geq 0$. Together with a convex and differentiable objective, the optimization can thus be solved efficiently in each iteration using the projection-free Frank-Wolfe procedure (Jaggi 2013). This process of computing the first eigenvector \mathbf{v} of a previous PSD solution \mathbf{M}_{t-1} to establish linear constraints $\lambda_{\min}^-(\mathbf{S}_t \mathbf{M} \mathbf{S}_t^{-1}) \geq 0$ in the next iteration, replacing the PSD cone constraint $\mathbf{M} \succeq 0$, is called *GDPA linearization*.

²A balanced graph has no cycles of odd number of negative edges. By the Cartwright-Harary Theorem, a graph is balanced iff nodes can be colored into red/blue, so that each positive/negative edge connects nodes of the same/different colors.

³A similarity transform $\mathbf{B} = \mathbf{SAS}^{-1}$ and the original matrix \mathbf{A} share the same set of eigenvalues (Varga 2004).

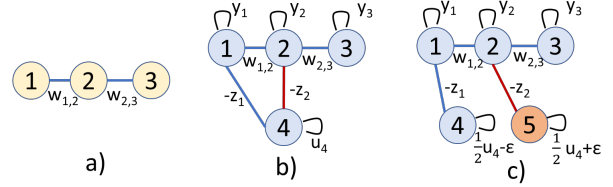


Figure 3: (a) An example 3-node line graph. (b) Unbalanced graph corresponding to solution \mathbf{H} to SDR dual (8) interpreted as graph Laplacian matrix. (c) Balanced graph corresponding to solution $\tilde{\mathbf{H}}$ to modified SDR dual (10) interpreted as Laplacian. Positive / negative edges are colored in blue / red. Self-loop weight u_4 in (b) for node 4 is $u_4 = y_4 + z_1 + z_2$.

GRAPH CLASSIFIER LEARNING

We first formulate the binary graph classifier learning problem and relax it to an SDP problem. We then present its SDP dual with dual variable matrix \mathbf{H} . Finally, we augment the SDP dual with variable $\tilde{\mathbf{H}}$, which is a graph Laplacian to a balanced graph, amenable to GDPA linearization.

SDP Primal

Given a PSD graph Laplacian matrix $\mathbf{L} \in \mathbb{R}^{N \times N}$ of a *positive* similarity graph \mathcal{G}^o (*i.e.*, $w_{i,j} \geq 0, \forall (i,j) \in \mathcal{E}$), we formulate a graph-based binary classification problem as

$$\min_{\mathbf{x}} \mathbf{x}^\top \mathbf{L} \mathbf{x}, \quad \text{s.t.} \quad \begin{cases} x_i^2 = 1, \forall i \in \{1, \dots, N\} \\ x_i = \hat{x}_i, \forall i \in \{1, \dots, M\} \end{cases} \quad (4)$$

where $\{\hat{x}_i\}_{i=1}^M$ are the M known binary labels. The quadratic objective in (4) is a GLR (1), promoting a label solution \mathbf{x} that is smooth w.r.t. graph \mathcal{G}^o specified by \mathbf{L} . The first constraint ensures x_i is binary, *i.e.*, $x_i \in \{-1, 1\}$. The second constraint ensures that entries in \mathbf{x} agree with known labels $\{\hat{x}_i\}_{i=1}^M$.

As an example, consider a 3-node line graph shown in Fig. 3(a), where edges (1, 2) and (2, 3) have weights $w_{1,2}$ and $w_{2,3}$, respectively. The corresponding adjacency and graph Laplacian matrices, \mathbf{W} and \mathbf{L} , are:

$$\mathbf{W} = \begin{bmatrix} 0 & w_{1,2} & 0 \\ w_{1,2} & 0 & w_{2,3} \\ 0 & w_{2,3} & 0 \end{bmatrix}, \quad \mathbf{L} = \begin{bmatrix} d_1 & -w_{1,2} & 0 \\ -w_{1,2} & d_2 & -w_{2,3} \\ 0 & -w_{2,3} & d_3 \end{bmatrix}$$

where $d_i = \sum_j w_{i,j}$ is the *degree* of node i . Suppose known labels are $\hat{x}_1 = 1$ and $\hat{x}_2 = -1$.

(4) is NP-hard due to the binary constraint. One can define a corresponding SDR problem as follows. Define first matrix $\mathbf{X} = \mathbf{x}\mathbf{x}^\top$, then $\mathbf{M} = [\mathbf{X} \ \mathbf{x}; \ \mathbf{x}^\top \ 1]$. \mathbf{M} is PSD because: i) block [1] is PSD, and ii) the *Schur complement* of block [1] of \mathbf{M} is $\mathbf{X} - \mathbf{x}\mathbf{x}^\top = \mathbf{0}$, which is also PSD. Thus, $\mathbf{X} = \mathbf{x}\mathbf{x}^\top$ (*i.e.*, $\text{rank}(\mathbf{X}) = 1$) implies $\mathbf{M} \succeq 0$. $\mathbf{X} = \mathbf{x}\mathbf{x}^\top$ and $X_{ii} = 1, \forall i$ together imply $x_i^2 = 1, \forall i$. To convexify the problem, we drop the non-convex rank constraint and write the SDR as

$$\min_{\mathbf{x}, \mathbf{X}} \text{Tr}(\mathbf{L}\mathbf{X}) \quad \text{s.t.} \quad \begin{cases} X_{ii} = 1, i \in \{1, \dots, N\} \\ \mathbf{M} \triangleq \begin{bmatrix} \mathbf{X} & \mathbf{x} \\ \mathbf{x}^\top & 1 \end{bmatrix} \succeq 0 \\ x_i = \hat{x}_i, i \in \{1, \dots, M\} \end{cases} \quad (5)$$

where $\text{Tr}(\mathbf{x}^\top \mathbf{L} \mathbf{x}) = \text{Tr}(\mathbf{L} \mathbf{x} \mathbf{x}^\top) = \text{Tr}(\mathbf{L} \mathbf{X})$. Because (5) has linear objective and constraints with an additional PSD cone

constraint, $\mathbf{M} \succeq 0$, it is an SDP problem. We call (5) the *SDR primal*.

Unfortunately, the solution \mathbf{M} to (5) is not a graph Laplacian matrix to a balanced graph, and hence GDPA linearization cannot be applied. Thus, we next investigate its SDP dual instead.

SDP Dual with Balanced Graph Laplacian

Following standard SDP duality theory (Gartner and Matussek 2012), we write the corresponding dual problem as follows. We first define

$$\mathbf{A}_i = \text{diag}(\mathbf{e}_{N+1}(i)), \quad \mathbf{B}_i = \begin{bmatrix} \mathbf{0}_{N \times N} & \mathbf{e}_N(i) \\ \mathbf{e}_N^\top(i) & 0 \end{bmatrix} \quad (6)$$

where $\mathbf{e}_N(i) \in \{0, 1\}^N$ is a length- N binary *canonical vector* with a single non-zero entry equals to 1 at the i -th entry, $\mathbf{0}_{N \times N}$ is a N -by- N matrix of zeros, and $\text{diag}(\mathbf{v})$ is a diagonal matrix with diagonal entries equal to \mathbf{v} .

Next, we put M known binary labels $\{\hat{x}_i\}_{i=1}^M$ into a vector $\mathbf{b} \in \mathbb{R}^M$ of length M ; specifically, we define

$$b_i = 2\hat{x}_i, \quad \forall i \in \{1, \dots, M\}. \quad (7)$$

We are now ready to write the SDR dual of (5) as

$$\begin{aligned} \min_{\mathbf{y}, \mathbf{z}} \quad & \mathbf{1}_{N+1}^\top \mathbf{y} + \mathbf{b}^\top \mathbf{z}, \\ \text{s.t.} \quad & \mathbf{H} \triangleq \sum_{i=1}^{N+1} y_i \mathbf{A}_i + \sum_{i=1}^M z_i \mathbf{B}_i + \mathbf{L}_{N+1} \succeq 0 \end{aligned} \quad (8)$$

where $\mathbf{1}_N$ is an all-one vector of length N , and $\mathbf{L}_{N+1} \triangleq [\mathbf{L} \ \mathbf{0}_{N \times 1}; \mathbf{0}_{1 \times N} \ 0]$. Variables to the dual (8) are $\mathbf{y} \in \mathbb{R}^{N+1}$ and $\mathbf{z} \in \mathbb{R}^M$.

Given the minimization objective, when $b_i < 0$, the corresponding z_i must be ≥ 0 , since $z_i < 0$ would make \mathbf{H} harder to be PSD (a larger Gershgorin disc radius) while worsening the objective. Similarly, for $b_i > 0$, $z_i \leq 0$. Thus, the signs of z_i 's are known beforehand. Without loss of generality, we assume $z_i \leq 0, \forall i \in \{1, \dots, M_1\}$ and $z_i \geq 0, \forall i \in \{M_1 + 1, \dots, M\}$ in the sequel.

Continuing our earlier 3-node graph example, solution \mathbf{H} to the SDP dual (8) is

$$\mathbf{H} = \begin{bmatrix} y_1 + d_1 & -w_{1,2} & 0 & z_1 \\ -w_{1,2} & y_2 + d_2 & -w_{2,3} & z_2 \\ 0 & -w_{2,3} & y_3 + d_3 & 0 \\ z_1 & z_2 & 0 & y_4 \end{bmatrix}. \quad (9)$$

The signed graph \mathcal{G} corresponding to \mathbf{H} —interpreted as a generalized graph Laplacian matrix—is shown in Fig. 3(b). We see that the first three nodes correspond to the three nodes in Laplacian \mathbf{L} with added self-loops of weights y_i 's. The last node has $M = 2$ edges with weights $-z_1$ and $-z_2$ to the first two nodes. Because of the edges from the last node have different signs to the first N nodes, \mathcal{G} is not balanced.

Reformulating the SDP Dual

We construct a balanced graph $\bar{\mathcal{G}}$ as an approximation to the imbalanced \mathcal{G} . This is done by splitting node $N + 1$ in \mathcal{G} into two in $\bar{\mathcal{G}}$, dividing positive and negative edges between them, as shown in Fig. 3. This results in $N + 2$ nodes for $\bar{\mathcal{G}}$. The specific graph construction for $\bar{\mathcal{G}}$ procedure is:

1. Construct first N nodes with the same edges as \mathcal{G} .
2. Construct node $N + 1$ with positive edges $\{-z_i\}_{i=1}^{M_1}$ and node $N + 2$ with negative edges $\{-z_i\}_{i=M_1+1}^M$ to the first N nodes in \mathcal{G} .
3. Add self-loops for node $N + 1$ and $N + 2$ with respective weights $\bar{u}_{N+1} = u_{N+1}/2 - \epsilon$ and $\bar{u}_{N+2} = u_{N+1}/2 + \epsilon$, where $\epsilon \in \mathbb{R}$ is a parameter.

Denote by $\bar{\mathbf{H}} \in \mathbb{R}^{(N+2) \times (N+2)}$ the generalized graph Laplacian matrix to augmented graph $\bar{\mathcal{G}}$. Continuing our example, Fig. 3(c) shows graph $\bar{\mathcal{G}}$. Corresponding $\bar{\mathbf{H}}$ is

$$\bar{\mathbf{H}} = \begin{bmatrix} y_1 + d_1 & -w_{1,2} & 0 & z_1 & 0 \\ -w_{1,2} & y_2 + d_2 & -w_{2,3} & 0 & z_2 \\ 0 & -w_{2,3} & y_3 + d_3 & 0 & 0 \\ z_1 & 0 & 0 & \bar{u}_4 + z_1 & 0 \\ 0 & z_2 & 0 & 0 & \bar{u}_5 + z_2 \end{bmatrix}.$$

where $\bar{u}_4 = u_4/2 - \epsilon$, $\bar{u}_5 = u_4/2 + \epsilon$, and $u_4 = y_4 + z_1 + z_2$. Spectrally, $\bar{\mathbf{H}}$ and \mathbf{H} are related; $\lambda_{\min}(\bar{\mathbf{H}}) \leq \lambda_{\min}(\mathbf{H})$. See (Yang et al. 2021) for a proof.

We reformulate the SDP dual (8) by keeping the same objective but imposing PSD cone constraint on $\bar{\mathbf{H}}$ instead, which implies a PSD \mathbf{H} . Define \mathbf{A}'_i , \mathbf{B}'_i and \mathbf{B}''_i similarly to (6) but for a larger $(N + 2)$ -by- $(N + 2)$ matrix; *i.e.*, $\mathbf{A}'_i = \text{diag}(\mathbf{e}_{N+2}(i))$, $\mathbf{B}'_i = [\mathbf{B}_i \ \mathbf{0}_{N+1}; \mathbf{0}_{N+1}^\top \ 0]$, and $\mathbf{B}''_i = [\mathbf{0}_{(N+1) \times (N+1)} \ \mathbf{e}_{N+1}(i); \mathbf{e}_{N+1}^\top(i) \ 0]$. The reformulated SDR dual is

$$\begin{aligned} \min_{\mathbf{y}, \mathbf{z}} \quad & \mathbf{1}_{N+1}^\top \mathbf{y} + \mathbf{b}^\top \mathbf{z}, \\ \text{s.t.} \quad & \bar{\mathbf{H}} \triangleq \sum_{i=1}^N y_i \mathbf{A}'_i + \kappa_{N+1} \mathbf{A}'_{N+1} + \kappa_{N+2} \mathbf{A}'_{N+2} \\ & + \sum_{i=1}^{M_1} z_i \mathbf{B}'_i + \sum_{i=M_1+1}^M z_i \mathbf{B}''_i - \mathbf{L} \succeq 0 \end{aligned} \quad (10)$$

where $\kappa_{N+1} = \frac{u_{N+1}}{2} - \sum_{i=1}^{M_1} z_i - \epsilon$ and $\kappa_{N+2} = \frac{u_{N+1}}{2} - \sum_{i=M_1+1}^M z_i + \epsilon$.

Given $\bar{\mathbf{H}}$ is now a Laplacian to a balanced graph, GDPA linearization can be applied to solve (10) efficiently. Specifically, in each iteration t , the first eigenvector \mathbf{v} of previous solution $\bar{\mathbf{H}}_{t-1}$ is computed using LOBPCG to define matrix $\mathbf{S}_t = \text{diag}(v_1^{-1}, \dots)$. \mathbf{S}_t is then used to define linear constraints $\lambda_{\min}(\mathbf{S}_t \bar{\mathbf{H}} \mathbf{S}_t^{-1}) \geq 0$, replacing $\bar{\mathbf{H}} \succeq 0$ in (10). This results in a LP, efficiently solvable using a state-of-the-art LP solver such as Simplex or interior point (Vanderbei 2021). The algorithm is run iteratively until convergence.

OPTIMIZING GRAPH PARAMETERS

After unrolling the iterative algorithm described above to solve (10) into a neural network architecture as shown in Fig. 1, we discuss next how to optimize parameters in each layer end-to-end via SGD for optimal performance. Specifically, we consider two methods—Mahalanobis distance learning and local linear embedding—to optimize graph edge weights, so that the most appropriate graph can be employed for classification in each layer.

Table 1: Trainable parameters for a P -layer network. M denotes the number of neurons in a dense layer.

method	trainable parameters	
	type	count
MLP/CNN/GCN	weights/bias	$M[M(P-1) + P + K + 2] + 2$
SDR	Q	$\leq PK(K+1)/2$
	$Q, \lambda, \mu, \alpha_i$	$\leq P(4 + K(K+1)/2)$

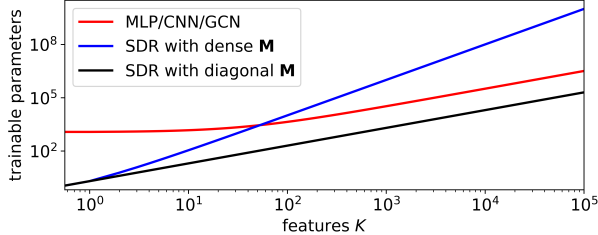


Figure 4: Trainable parameters when the number of layers $P = 2$ and number of neurons $M = 32$ in a dense layer of a black-box network. Our SDR can have trainable parameters close to $\mathcal{O}(K)$ (i.e., a line that leans towards the black line) with a sparsity pattern constraint.

Mahalanobis Distance Learning

We assume that edge weight $w_{i,j}$ between nodes i and j is inversely proportional to *feature distance* $d_{i,j}$, computed using a Gaussian kernel, i.e.,

$$w_{i,j} = \exp\left(-\frac{d_{i,j}}{\sigma_d^2}\right). \quad (11)$$

Using an exponential kernel for $d_{i,j} \in [0, \infty)$ means $w_{i,j} \in (0, 1]$, which ensures a positive graph as required in (4).

We optimize feature distance $d_{i,j}$ in each neural layer as follows. Assuming each node i is endowed with a feature vector $\mathbf{f}_i \in \mathbb{R}^K$ of dimension K , $d_{i,j}$ can be computed as the *Mahalanobis distance* (Mahalanobis 1936) using a PSD *metric matrix* $\mathbf{M} \succeq 0$:

$$d_{i,j} = (\mathbf{f}_i - \mathbf{f}_j)^\top \mathbf{M} (\mathbf{f}_i - \mathbf{f}_j). \quad (12)$$

\mathbf{M} can be decomposed into $\mathbf{M} = \mathbf{Q}\mathbf{Q}^\top$ via *Cholesky factorization* (Golub and Van Loan 1996), where \mathbf{Q} is a lower triangular matrix. In each neural layer, we first initialize an empirical covariance matrix \mathbf{E} using available feature vectors $\{\mathbf{f}_i\}$. We then apply Cholesky factorization to $\mathbf{E}^{-1} = \mathbf{Q}\mathbf{Q}^\top$. Next, we designate a sparsity pattern in \mathbf{Q} by setting to zero entries in \mathbf{Q} whose amplitudes are small than factor $\zeta > 0$ times the average of the diagonals in \mathbf{Q} . Table 1 and Fig. 4 show the number of trainable parameters for a P -layer unrolled network. With a sparsity pattern set by a carefully chosen ζ , the number of trainable parameters in \mathbf{Q} in our network is $\mathcal{O}(K)$.

Using computed edge weights in (11), one can compute a graph Laplacian matrix $\mathbf{L}_1 = \text{diag}(\mathbf{W}\mathbf{1}) - \mathbf{W}$, where $\mathbf{1}$ is the all-one vector.

Local Linear Embedding

We compute a second graph Laplacian matrix \mathbf{L}_2 via *local linear embedding* (LLE) (Roweis and Saul 2000; Ghojogh

et al. 2020). Specifically, we compute a *sparse* coefficient matrix $\mathbf{C} \in \mathbb{R}^{N \times N}$, so that each feature vector $\mathbf{f}_i \in \mathbb{R}^K$ can be represented as a sparse linear combination of other feature vectors $\mathbf{f}_j, \forall j | j \neq i$. We first define matrix $\mathbf{F} \triangleq [\mathbf{f}_1; \dots; \mathbf{f}_K] \in \mathbb{R}^{N \times K}$ that contains feature vector \mathbf{f}_i as row i . We then formulate the following group sparsity problem:

$$\min_{\mathbf{C} \in \mathcal{S}^+} \|\mathbf{F} - \mathbf{C}\mathbf{F}\|_2^2 + \eta \|\mathbf{C}\|_{1,1} \quad (13)$$

where \mathcal{S}^+ is the set of symmetric matrices with zero diagonal terms and non-negative off-diagonal terms, and $\eta > 0$ is a parameter that induces sparsity in \mathbf{C} . Matrix symmetry and non-negativity are enforced, so that bi-directional positive edge weights can be easily deduced from \mathbf{C} . Using non-negative weights for LLE is called *non-negative kernel regression* (NNK) in (Shekizhar and Ortega 2020).

The objective in (13) contains two convex terms, where only the first term is differentiable. Thus, we optimize (13) iteratively using *proximal gradient* (PG) (Parikh and Boyd 2013) given an initial matrix \mathbf{C} that corresponds to the adjacency matrix of a k -nearest neighbor graph as input. Specifically, at each iteration t , we first optimize the first term $\|\mathbf{F} - \mathbf{C}\mathbf{F}\|_2^2$ via gradient descent with step size δ . We then optimize the second term via soft-thresholding $T(c_{i,j})$:

$$T(c_{i,j}) = \begin{cases} c_{i,j} - \eta & \text{if } c_{i,j} \geq \eta \\ 0 & \text{o.w.} \end{cases} \quad (14)$$

$T(\cdot)$ combines the proximal operator for the ℓ_1 -norm and the projection operator onto \mathcal{S}^+ .

As done in (He et al. 2019; Ghojogh et al. 2020), the weights of the optimized \mathbf{C} can be further adjusted using known labels in a semi-supervised manner: the weights for the same-label (different-label) sample pairs are increased by parameter $\gamma > 0$ (decreased by parameter $\mu > 0$).

After \mathbf{C} is obtained, we interpret it as an adjacency matrix and compute its corresponding graph Laplacian matrix $\mathbf{L}_2 = \text{diag}(\mathbf{C}\mathbf{1}) - \mathbf{C}$. Finally, we compute a new graph Laplacian \mathbf{L} as a *conic combination* of \mathbf{L}_1 computed via feature distance specified by metric matrix \mathbf{M} and \mathbf{L}_2 computed via LLE specified by coefficient matrix \mathbf{C} , i.e.,

$$\mathbf{L} = \alpha_1 \mathbf{L}_1 + \alpha_2 \mathbf{L}_2, \quad \alpha_i \geq 0. \quad (15)$$

$\alpha_i \geq 0$ ensures that the conically combined \mathbf{L} is a Laplacian for a positive graph. Trainable parameters for \mathbf{L} consist of the two LLE adjustment parameters (γ and μ) and the two Laplacian weight parameters (α_1 and α_2).

Loss Function and Inference

As shown in Fig. 1, we train parameters $\mathbf{Q}, \gamma, \mu, \alpha_1$ and α_2 in each SDR layer in an end-to-end fashion via backpropagation (Rumelhart, Hinton, and Williams 1986). During training, a mean-squared-error (MSE) loss function is defined as

$$L = \left\| g \left[f_P \left(f_{P-1} \left(\dots f_1(\mathbf{Q}, \alpha_i, \gamma, \mu, \mathbf{y}, \mathbf{z}) \right) \right) \right] - \hat{\mathbf{x}}_{\{M+1, \dots, N\}} \right\|_2^2, \quad (16)$$

where $g[\cdot] \triangleq \text{sign} \{ \hat{x}_1 v_1 \mathbf{v}_{\{M+1, \dots, N\}} \}$ is the label prediction equation, \mathbf{v} is the first eigenvector of \mathbf{H} computed by

LOBPCG, and $f_P(f_{P-1}(\dots))$ are nested differentiable functions corresponding to the P -layers in our unrolled network. (16) is essentially the MSE loss of entries $M + 1$ to N of \mathbf{x} (unknown labels) compared to the ground-truth labels. We optimize the parameters using an off-the-shelf SGD optimizer.

During inference, test data is passed through the unrolled network, where the optimized \mathbf{Q} , γ , μ , α_1 and α_2 are fixed. \mathbf{Q} is used to define the metric matrix \mathbf{M} to construct \mathbf{L}_1 . γ and μ are used to construct \mathbf{L}_2 together with the LLE weight matrix \mathbf{C} learned from the test data via (13). α_1 and α_2 are used to define \mathbf{L} . Finally, unknown labels are predicted.

EXPERIMENTS

Experimental Setup

We implemented our unrolled network in PyTorch⁴, and evaluated it in terms of average classification error rate and inference runtime. We compared our algorithm against the following six model-based schemes: i) a primal-dual interior-point solver that solves the SDP primal in Eq. (5), MOSEK, available in CVX with a Professional license (CVX 2020); ii) a biconvex relaxation solver BCR (Shah et al. 2016; BCR 2020); iii) a spectrahedron-based relaxation solver SD-Cut (Wang, Shen, and van den Hengel 2013; Wang et al. 2017; SDcut 2013) that involves L-BFGS-B (Zhu et al. 1997); iv) an ADMM first-order operator-splitting solver CDCS (Zheng, Fantuzzi, and Papachristodoulou 2019; Zheng et al. 2020) with an LGPL-3.0 License (CDCS 2016) that solves the modified SDP dual in Eq. (10); v) a graph Laplacian regularizer GLR (Pang and Cheung 2017) with a box constraint $x_i \in [-1, 1]$ for predicted labels; and vi) baseline model-based version of our SDR network proposed in (Yang et al. 2021) based on GDPA (Yang, Cheung, and Hu 2021).

In addition, we compared our network against four neural network schemes: vii) an unrolled 1-layer SDP classifier network that solves (10) using a differentiable SDP solver in a Cvxpylayer library (Agrawal et al. 2019; Agrawal and Boyd 2020); viii) a multi-layer perceptron (MLP) consisted of two dense layers; ix) a convolutional neural network (CNN) consisted of two 1-D convolutional layers (each with a kernel size 1 and stride 2); and x) a graph convolutional network (GCN) (Kipf and Welling 2017) consisted of two graph convolutional layers. For GCN, the adjacency matrix is computed in the same way as the one used to compute the graph Laplacian in (1) and is fixed throughout the network training procedure. For MLP, CNN and GCN, each (graph) convolutional layer is consisted of 32 neurons and is followed by group normalization (Wu and He 2018), rectified linear units (Fukushima 1969) and dropout (Srivastava et al. 2014) with a rate 0.2. A 1-D max-pooling operation with a kernel size 1 and stride 2 is placed before the dropout for CNN. A cross entropy loss based on the log-softmax (de Brébisson and Vincent 2016) is adopted for MLP, CNN and GCN.

We set the sparsity factor as $\zeta = 0.9$ to initial lower triangular \mathbf{Q} , the sparsity weight parameter as $\eta = 0.01$ in (14), the Laplacian weight parameter in (15) as $\alpha_1 = \alpha_2 = 1$, and the LLE weight adjustment parameters as $\gamma = 1$ and

⁴results reproducible via code in https://anonymous.4open.science/r/SDP_RUN-4D07/.

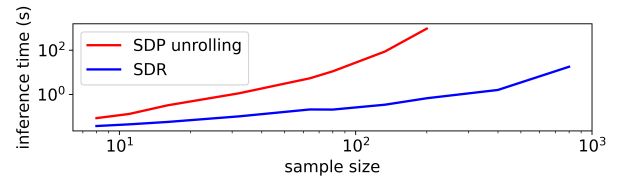


Figure 5: Inference time of SDR v.s. naive SDP unrolling. Our speedup is over 1400 \times when the sample size is 200.

$\mu = 1$. We set the convergence threshold of i) LOBPCG to 10^{-4} with 200 maximum iterations, ii) the differentiable LP solver to 10^{-6} with 1000 maximum iterations. We set the learning rate for the SGD optimizer used in all methods to 10^{-2} . The maximum iterations for the optimization of \mathbf{Q} and \mathbf{C} was set to 1000 for the pure model-based methods i, iii, iv, v and vi that involve graph construction. For fast convergence, we set the convergence thresholds of CDCS and SDCut to 10^{-3} , the maximum ADMM iterations in CDCS to 1000, the maximum iterations for L-BFGS-B in SDCut and the main loop in BCR to 100, and the Frobenius norm weight in SDCut to 100. The number of epochs for the three data-driven networks, viii, ix and x, was set to 1000. For the SDP unrolled network vii and our unrolled network it was 20. All computations were carried out on a Ubuntu 20.04.2 LTS PC with AMD Ryzen Threadripper 3960X 24-core processor 3.80 GHz and 128GB of RAM.

We employed 17 binary datasets freely available from UCI (UCI 2021) and LibSVM (LibSVM 2021). For efficiency, we first performed a K -fold ($K \leq 9$) split for each dataset with random seed 0, and then created 5 instances of 80% training-20% test split for each fold, with random seeds 1-5 (Russell and Norvig 2009). For the six model-based approach and the three data-driven networks, the ground-truth labels for the above 80% training data were used for semi-supervised graph classifier learning (Yang et al. 2021) and supervised network training. For our SDR unrolled network, we further created a 75% unroll-training-25% unroll-test split for the 80% training data, where, first, the ground-truth labels for the unroll-training data were used for the semi-supervised SDR network training together with the unroll-test data, and second, the learned parameters were used for label inference of the remaining 20% test data. The above setup resulted in sample sizes from 62 to 292. We applied a *standardization* data normalization scheme in (Dong et al. 2020) that first subtracts the mean and divides by the feature-wise standard deviation, and then normalizes to unit length sample-wise. We added 10^{-12} noise to the dataset to avoid NaN's due to data normalization on small samples.

Experimental Results

We first show in Fig. 5 the inference runtime of our SDR network compared to a SDP unrolled network that naively unrolls the PSD cone projection using the same Cvxpylayer python library described earlier. It is clear that our SDR network is substantially faster in inference than the naïve SDP unrolled network, with a speedup that is over 1400 \times when the sample size is 200.

We next show in Table 2 the classification error rates of

Table 2: Classification error rates (%). K denotes feature count.

dataset	K	model-based						neural nets					
		MOSEK	BCR	SDcut	CDCS	GLR	GDPA	MLP	CNN	GCN	SDR T	SDR Q	SDR Q+LLE
australian	14	20.14	15.65	15.65	15.65	16.67	15.51	17.39	17.83	19.57	18.70	15.65	16.95
breast-cancer	10	3.85	3.41	3.56	3.41	4.30	3.56	5.19	4.89	12.59	3.48	3.48	5.33
diabetes	8	35.16	32.94	31.76	31.63	33.59	35.03	32.31	36.15	33.08	30.98	30.00	29.62
fourclass	2	28.30	23.98	23.51	23.51	25.38	25.03	26.08	25.15	25.15	29.77	27.93	27.12
german	24	26.90	26.90	26.90	27.00	26.90	26.90	31.60	28.80	24.40	25.60	24.40	23.20
haberman	3	23.61	23.61	23.61	23.61	23.61	23.61	27.10	29.68	28.71	23.55	22.58	22.90
heart	13	20.37	18.89	18.89	18.89	18.52	18.89	24.81	24.07	23.70	17.41	18.89	21.11
ILPD	10	28.10	28.10	28.10	28.10	28.10	31.21	26.78	27.97	30.00	29.31	28.62	25.34
liver-disorders	5	30.00	27.86	30.71	30.00	29.29	30.71	37.86	39.29	44.29	41.33	36.00	34.67
monk1	6	29.82	26.25	26.07	27.86	26.43	26.07	6.43	5.71	12.86	32.73	26.18	27.64
pima	8	35.16	32.68	31.90	32.03	33.59	36.47	33.08	32.69	35.00	31.37	28.08	29.62
planning	12	25.00	25.00	25.00	25.00	25.00	25.00	39.44	40.56	33.89	25.41	24.86	23.78
voting	16	11.40	10.70	10.70	12.09	11.40	10.70	3.95	2.79	10.47	10.93	3.72	4.19
WDBC	30	7.54	7.72	7.54	8.07	7.37	7.54	4.64	4.46	22.86	9.47	7.14	6.79
sonar	60	31.90	23.33	21.90	21.90	23.33	21.90	17.62	17.14	40.95	14.63	20.00	19.05
madelon	500	49.75	44.44	48.94	48.84	48.79	48.59	46.82	47.78	46.11	41.92	43.59	40.76
colon-cancer	2000	38.33	36.67	38.33	38.33	38.33	38.33	28.33	26.67	38.33	32.31	28.33	23.08
avg.	—	26.20	24.01	24.30	24.47	24.74	25.00	24.08	24.21	28.35	24.64	22.91	22.42

the six model-based schemes, namely MOSEK, BCR, SDcut, CDCS, GLR and GDPA, the three data-driven networks, namely MLP, CNN and GCN, and the three variants of our SDR network where a single SDR layer optimizes i) a $K \times J$ matrix \mathbf{T} for $\mathbf{M} = \mathbf{T}\mathbf{T}^\top$ where $J = 2$ is the pre-defined rank, ii) our proposed lower-triangular matrix \mathbf{Q} sparsified by ζ , and iii) \mathbf{Q} plus LLE weight adjustment parameters γ and μ and Laplacian weighting parameters α_1 and α_2 .

We first observe that, in general, with an appropriate choice of the trainable parameters, SDR \mathbf{Q} and SDR \mathbf{Q} +LLE outperformed on average all model-based schemes and were competitive with data-driven schemes. SDR \mathbf{Q} +LLE on average performed better than SDR \mathbf{Q} thanks to the four additional trainable parameters γ , μ , α_1 and α_2 .

We observe also that the three data-driven schemes, MLP, CNN and GCN, performed on average slightly worse than SDR \mathbf{Q} and SDR \mathbf{Q} +LLE. This can be explained by the relatively large number of trainable parameters that may cause overfitting. For example, MLP is consisted of 1602 trainable parameters with 32 neurons in each of the two dense layers during training on the dataset `australian`, while 1-layer SDR \mathbf{Q} and SDR \mathbf{Q} +LLE have at most 105 and 109 trainable parameters, respectively. We see also that SDR \mathbf{T} , SDR \mathbf{Q} and SDR \mathbf{Q} +LLE learned faster than the three data-driven schemes with only 20 epochs in training stage compared to 1000 epochs for MLP, CNN and GCN. We note further that our unrolled network is by design more interpretable than the three generic black box data-driven implementations, where each neural layer is an iteration of an iterative algorithm.

We observe that SDR \mathbf{Q} and SDR \mathbf{Q} +LLE outperformed SDR \mathbf{T} , demonstrating that our proposed parameterization of graph edge weights at each neural layer is better than simple low-rank factorization $\mathbf{M} = \mathbf{T}\mathbf{T}^\top$. For SDR \mathbf{T} , SDR \mathbf{Q} and SDR \mathbf{Q} +LLE, the noticeably worse performance on the

Table 3: Classification error rates (%) on the dataset `sonar` using our SDR \mathbf{Q} +LLE with P layers.

P	1	2	3
error rate (%)	19.05	16.59	16.10

dataset `liver-disorders` compared to the model-based schemes may be explained by the fact that the optimizer was stuck at a bad local minimum.

We show in Table 3 the classification error rate of our SDR \mathbf{Q} +LLE with 1, 2 and 3 SDR layers on the dataset `sonar`. We see that as the number of layers P increases, the classification error rates are reduced at the cost of introducing more network parameters. This indicates that our SDR network is resilient to overfitting when the number of trainable parameters increases by a factor of P .

CONCLUSION

To facilitate algorithm unfolding of a proximal splitting algorithm that requires PSD cone projection, using binary graph classifier as an illustrative example, we propose an unrolling strategy via GDPA linearization. Specifically, we replace the PSD cone constraint in the semi-definite programming relaxation (SDR) of the classifier problem by “tight possible” linear constraints per iteration, so that each iteration requires only computing a linear program (LP) and the first eigenvector of the previous matrix solution. After unrolling iterations of the projection-free algorithm into neural layers, we optimize parameters that determine graph edge weights in each layer via stochastic gradient descent (SGD). Experiments show that our unrolled network outperformed pure model-based classifiers, and had comparable performance as pure data-driven schemes while employing far fewer parameters.

References

- [Agrawal and Boyd 2020] Agrawal, A., and Boyd, S. 2020. Differentiating through log-log convex programs. *arXiv*.
- [Agrawal et al. 2019] Agrawal, A.; Amos, B.; Barratt, S.; Boyd, S.; Diamond, S.; and Kolter, Z. 2019. Differentiable convex optimization layers. In *Advances in Neural Information Processing Systems*.
- [BCR 2020] BCR. 2020. BCR implementation. https://github.com/Axeldnahcram/biconvex_relaxation. Accessed: 2021-9-6.
- [Beck and Teboulle 2009] Beck, A., and Teboulle, M. 2009. A fast iterative shrinkage-thresholding algorithm for linear inverse problems. *SIAM J. Imaging Sci.* 2:183–202.
- [Belkin, Matveeva, and Niyogi 2004] Belkin, M.; Matveeva, I.; and Niyogi, P. 2004. Regularization and semisupervised learning on large graphs. In *Shawe-Taylor J., Singer Y. (eds) Learning Theory, COLT 2004, Lecture Notes in Computer Science*, volume 3120, 624–638.
- [Bottou 1998] Bottou, L. 1998. Online algorithms and stochastic approximations. In Saad, D., ed., *Online Learning and Neural Networks*. Cambridge, UK: Cambridge University Press. revised, oct 2012.
- [Boyd et al. 2011] Boyd, S.; Parikh, N.; Chu, E.; Peleato, B.; and Eckstein, J. 2011. Distributed optimization and statistical learning via the alternating direction method of multipliers. In *Foundations and Trends in Optimization*, volume 3, no.1, 1–122.
- [Cartwright and Harary 1956] Cartwright, D., and Harary, F. 1956. Structural balance: a generalization of Heider’s theory. In *Psychological Review*, volume 63, no.5, 277–293.
- [CDCS 2016] CDCS. 2016. CDCS implementation. <https://github.com/oxfordcontrol/CDCS>. Accessed: 2021-9-6.
- [CVX 2020] CVX. 2020. CVX Research. <http://cvxr.com/cvx/>. Accessed: 2021-9-6.
- [de Brébisson and Vincent 2016] de Brébisson, A., and Vincent, P. 2016. An exploration of softmax alternatives belonging to the spherical loss family. In *International Conference on Learning Representations*.
- [Dong et al. 2020] Dong, M.; Wang, Y.; Yang, X.; and Xue, J. 2020. Learning local metrics and influential regions for classification. *IEEE TPAMI* 42(6):1522–1529.
- [Fukushima 1969] Fukushima, K. 1969. Visual feature extraction by a multilayered network of analog threshold elements. *IEEE Transactions on Systems Science and Cybernetics* 5(4):322–333.
- [Gartner and Matousek 2012] Gartner, B., and Matousek, J. 2012. *Approximation Algorithms and Semidefinite Programming*. Springer.
- [Ghohogh et al. 2020] Ghohogh, B.; Ghodsi, A.; Karray, F.; and Crowley, M. 2020. Locally linear embedding and its variants: Tutorial and survey.
- [Golub and Van Loan 1996] Golub, G. H., and Van Loan, C. F. 1996. *Matrix Computations*. The Johns Hopkins University Press, third edition.
- [Gregor and LeCun 2010] Gregor, K., and LeCun, Y. 2010. Learning fast approximations of sparse coding. In *International Conference on Machine Learning, ICML’10*, 399–406.
- [Guillory and Bilmes 2009] Guillory, A., and Bilmes, J. 2009. Label selection on graphs. In *Twenty-Third Annual Conference on Neural Information Processing Systems*.
- [He et al. 2019] He, P.; Jing, T.; Xu, X.; Zhang, L.; Liao, Z.; and Fan, B. 2019. Nonlinear manifold classification based on lle. In Bhatia, S. K.; Tiwari, S.; Mishra, K. K.; and Trivedi, M. C., eds., *Advances in Computer Communication and Computational Sciences*, 227–234. Singapore: Springer Singapore.
- [Helmberg et al. 1996] Helmberg, C.; Rendl, F.; Vanderbei, R.; and Wolkowicz, H. 1996. An interior-point method for semidefinite programming. In *SIAM J. Optim.*, volume 6, no.2, 342–361.
- [Jaggi 2013] Jaggi, M. 2013. Revisiting Frank-Wolfe: Projection-free sparse convex optimization. In *International Conference on Machine Learning*, 427–435.
- [Kipf and Welling 2017] Kipf, T. N., and Welling, M. 2017. Semi-Supervised Classification with Graph Convolutional Networks. In *International Conference on Learning Representations*.
- [Knyazev 2001] Knyazev, A. V. 2001. Toward the optimal preconditioned eigensolver: Locally optimal block preconditioned conjugate gradient method. *SIAM Journal on Scientific Computing* 23(2):517–541.
- [Krizhevsky, Sutskever, and Hinton 2012] Krizhevsky, A.; Sutskever, I.; and Hinton, G. E. 2012. Imagenet classification with deep convolutional neural networks. In *Advances in Neural Information Processing Systems*, volume 25.
- [LeCun, Bengio, and Hinton 2015] LeCun, Y.; Bengio, Y.; and Hinton, G. 2015. Deep learning. *Nature* 521(7553):436–444.
- [Li, Liu, and Tang 2008] Li, Z.; Liu, J.; and Tang, X. 2008. Pairwise constraint propagation by semidefinite programming for semi-supervised classification. In *ACM International Conference on Machine Learning*.
- [LibSVM 2021] LibSVM. 2021. LibSVM Data: Classification (Binary Class). <https://www.csie.ntu.edu.tw/~cjlin/libsvmtools/datasets/binary.html>. Accessed: 2021-9-6.
- [Luo et al. 2010] Luo, Z.; Ma, W.; So, A. M.; Ye, Y.; and Zhang, S. 2010. Semidefinite relaxation of quadratic optimization problems. *IEEE Signal Processing Magazine* 27(3):20–34.
- [Mahalanobis 1936] Mahalanobis, P. C. 1936. On the generalized distance in statistics. *Proceedings of the National Institute of Sciences of India* 2(1):49–55.
- [Monga, Li, and Eldar 2021] Monga, V.; Li, Y.; and Eldar, Y. C. 2021. Algorithm unrolling: Interpretable, efficient deep learning for signal and image processing. *IEEE Signal Processing Magazine* 38(2):18–44.
- [Moutafis, Leng, and Kakadiaris 2017] Moutafis, P.; Leng, M.; and Kakadiaris, I. A. 2017. An overview and empiri-

- cal comparison of distance metric learning methods. *IEEE Transactions on Cybernetics* 47(3):612–625.
- [O’Donoghue et al. 2016] O’Donoghue, B.; Chu, E.; Parikh, N.; and Boyd, S. 2016. Conic optimization via operator splitting and homogeneous self-dual embedding. In *Journal of Optimization Theory and Applications*, volume 169, no.3, 1042–1068.
- [Ortega et al. 2018] Ortega, A.; Frossard, P.; Kovacevic, J.; Moura, J. M. F.; and Vandergheynst, P. 2018. Graph signal processing: Overview, challenges, and applications. In *Proceedings of the IEEE*, volume 106, no.5, 808–828.
- [Pang and Cheung 2017] Pang, J., and Cheung, G. 2017. Graph Laplacian regularization for inverse imaging: Analysis in the continuous domain. In *IEEE Transactions on Image Processing*, volume 26, no.4, 1770–1785.
- [Parikh and Boyd 2013] Parikh, N., and Boyd, S. 2013. Proximal algorithms. In *Foundations and Trends in Optimization*, volume 1, no.3, 123–231.
- [Roweis and Saul 2000] Roweis, S., and Saul, L. 2000. Non-linear dimensionality reduction by locally linear embedding. *Science* 290 5500:2323–6.
- [Rumelhart, Hinton, and Williams 1986] Rumelhart, D. E.; Hinton, G. E.; and Williams, R. J. 1986. Learning Representations by Back-propagating Errors. *Nature* 323(6088):533–536.
- [Russell and Norvig 2009] Russell, S., and Norvig, P. 2009. *Artificial Intelligence: A Modern Approach*. USA: Prentice Hall Press, 3rd edition.
- [SDcut 2013] SDcut. 2013. SDcut implementation. <https://github.com/chhshen/SDCut>. Accessed: 2021-9-6.
- [Shah et al. 2016] Shah, S.; Kumar, A.; Castillo, C.; Jacobs, D.; Studer, C.; and Goldstein, T. 2016. Biconvex relaxation for semidefinite programming in computer vision. In *European Conference on Computer Vision*.
- [Shekkizhar and Ortega 2020] Shekkizhar, S., and Ortega, A. 2020. Graph construction from data using non negative kernel regression (NNK graphs). In *IEEE International Conference on Acoustics, Speech and Signal Processing*.
- [Shlezinger et al. 2021] Shlezinger, N.; Whang, J.; Eldar, Y. C.; and Dimakis, A. G. 2021. Model-based deep learning.
- [Srivastava et al. 2014] Srivastava, N.; Hinton, G.; Krizhevsky, A.; Sutskever, I.; and Salakhutdinov, R. 2014. Dropout: A simple way to prevent neural networks from overfitting. *J. Mach. Learn. Res.* 15(1):1929–1958.
- [UCI 2021] UCI. 2021. UCI machine learning repository. <https://archive.ics.uci.edu/ml/datasets.php>. Accessed: 2021-9-6.
- [Vanderbei 2021] Vanderbei, R. 2021. *Linear Programming: Foundations and Extensions (5th Edition)*. Springer Nature.
- [Varga 2004] Varga, R. S. 2004. *Gershgorin and his circles*. Springer.
- [Wang et al. 2017] Wang, P.; Shen, C.; Hengel, A.; and Torr, P. 2017. Large-scale binary quadratic optimization using semidefinite relaxation and applications. *IEEE Transactions on Pattern Analysis and Machine Intelligence* 39(3):470–485.
- [Wang, Shen, and van den Hengel 2013] Wang, P.; Shen, C.; and van den Hengel, A. 2013. A fast semidefinite approach to solving binary quadratic problems. In *IEEE International Conference on Computer Vision and Pattern Recognition*.
- [Wu and He 2018] Wu, Y., and He, K. 2018. Group normalization. In *ECCV*.
- [Yang et al. 2021] Yang, C.; Cheung, G.; tian Tan, W.; and Zhai, G. 2021. Projection-free graph-based classifier learning using Gershgorin disc perfect alignment. *arXiv*.
- [Yang, Cheung, and Hu 2021] Yang, C.; Cheung, G.; and Hu, W. 2021. Signed graph metric learning via Gershgorin disc perfect alignment. *arXiv*.
- [Zhang et al. 2017] Zhang, K.; Zuo, W.; Gu, S.; and Zhang, L. 2017. Learning deep cnn denoiser prior for image restoration. In *Proceedings of the IEEE Conference on Computer Vision and Pattern Recognition (CVPR)*.
- [Zheng et al. 2020] Zheng, Y.; Fantuzzi, G.; Papachristodoulou, A.; Goulyart, P.; and Wynn, A. 2020. Chordal decomposition in operator-splitting methods for sparse semidefinite programs. *Mathematical Programming* 180:489—532.
- [Zheng, Fantuzzi, and Papachristodoulou 2019] Zheng, Y.; Fantuzzi, G.; and Papachristodoulou, A. 2019. Fast ADMM for sum-of-squares programs using partial orthogonality. *IEEE Transactions on Automatic Control* 64(9):3869–3876.
- [Zhou et al. 2003] Zhou, D.; Bousquet, O.; Lal, T. N.; Weston, J.; and Scholkopf, B. 2003. Learning with local and global consistency. In *16th International Conference on Neural Information Processing (NIPS)*.
- [Zhu et al. 1997] Zhu, C.; Byrd, R.; Lu, P.; and Nocedal, J. 1997. Algorithm 778: L-BFGS-B: Fortran subroutines for large-scale bound-constrained optimization. *ACM Trans. Math. Softw.* 23(4):550–560.